

Templated Synthesis of Single-Component Polymer Capsules and Their Application in Drug Delivery

Yajun Wang,[†] Vipul Bansal,[†] Alexander N. Zelikin, and Frank Caruso*

Centre for Nanoscience and Nanotechnology, Department of Chemical and Biomolecular Engineering, The University of Melbourne, Victoria 3010, Australia

Received March 27, 2008; Revised Manuscript Received May 1, 2008

ABSTRACT

We report a general and facile approach for the fabrication of a new class of monodispersed, single-component and thick-walled polymer nanocapsules via the single-step assembly of macromolecules in solid core/mesoporous shell (SC/MS) silica particle templates, followed by cross-linking of the macromolecules and removal of the SC/MS templates. The general applicability of this approach is demonstrated by the preparation of nanocapsules using various polymers, including synthetic polyelectrolytes, polypeptides, and polypeptide–drug conjugates. The potential of doxorubicin (Dox)-loaded poly(L-glutamic acid) nanocapsules in tumor therapy applications is demonstrated via in vitro degradation experiments, which show a near-linear release of the Dox in the presence of a lysosomal hydrolase, nanocapsule uptake by human colorectal tumor cells, and delivery of the anticancer drug into the tumor cells, leading to tumor cell death.

During the past few decades, growing interest has been devoted to the design of delivery vehicles for transporting anticancer drugs to tumor sites. The use of polymer-based materials has played an important role in the development of such systems, largely because of the ability to prepare polymers with tailored properties, including biocompatibility, size, structure, and functionality. Several polymer-based vehicles have been reported, including polymer particles, polymer-based micelles, polymer–drug conjugates, and polymer nanocapsules. These systems can facilitate higher payloads,¹ prolong the circulation time of the drugs,^{1,2} improve drug targeting and solubility,^{1,2} and provide controlled release of the therapeutics into the blood stream or the targeted tumor tissues.^{1,3} Self-assembly^{4,5} and layer-by-layer (LbL) assembly^{6–10} processes have been widely used to prepare polymer capsules with well-defined chemical and structural properties. In LbL assembly, a sacrificial colloidal template is used to sequentially deposit multiple polymer layers, followed by removal of the core, leading to polymer capsules. Nonporous colloidal particles^{6,8–10} are commercially available with near-monodisperse size distributions in a wide range of sizes, from tens of nanometers to several micrometers, and are convenient templates to yield well-defined capsules with nanometer-thick walls. In contrast, porous particle templates^{11–14} allow polymer chains to infiltrate into the core and, upon core dissolution, give rise to nanoporous polymer particles. Such nanoporous polymer particles can

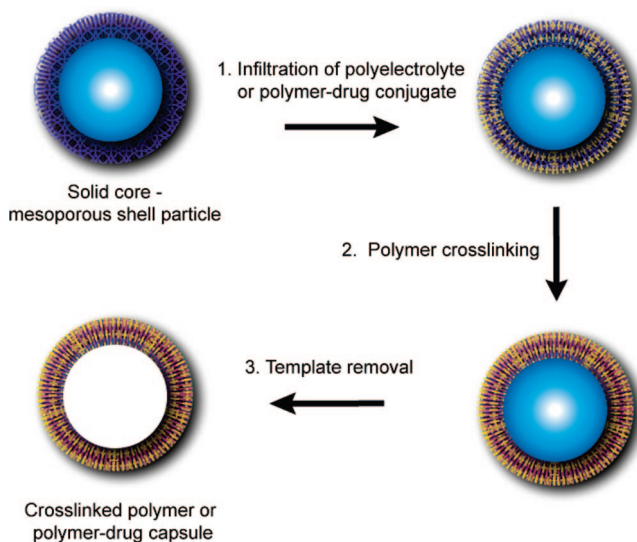
be exploited to load high quantities of drugs/proteins. In this study, we use solid core and mesoporous shell template particles^{15–18} to combine the versatility and benefits of the solid core particles and the high loading of nanoporous shells to prepare thick-walled, single-component polymer nanocapsules with controlled drug payload. The solid core/mesoporous shell (SC/MS) particles can be prepared with different particle size, shell thickness,¹⁶ and solid core composition (silica, gold, and Fe₃O₄ nanoparticles^{17,18}).

We used SC/MS particles with a solid silica core (ca. 300 nm) and mesoporous silica shell (ca. 60 nm) as templates. The macromolecules were assembled in the SC/MS template particles by solution adsorption, followed by covalent cross-linking of the macromolecules in the mesoporous silica shells, and subsequent removal of the SC/MS templates, resulting in polymer nanocapsules (Scheme 1). This approach offers a number of distinct advantages over the conventional LbL technique to prepare capsules. First, uniform nanocapsules of various macromolecules are obtained by a single macromolecular assembly step of a single macromolecule type, eliminating the need for multiple polymers and/or multiple polymer adsorption steps, which are typically required in conventional LbL assembly. Second, the nanocapsules derived from the SC/MS templates have porous walls that are significantly thicker than those prepared by LbL assembly (e.g., more than an order of magnitude for a single adsorption step), thus offering a simple approach to regulate the physical properties (e.g., structure, permeability) of the nanocapsules. Furthermore, the macromolecules as-

* Corresponding author, fcaruso@unimelb.edu.au.

[†] Y.W. and V.B. contributed equally to the work presented in this paper.

Scheme 1. Schematic Representation of the Preparation of Single-Component Macromolecular Capsules by Using Solid Core and Mesoporous Shell (SC/MS) Silica Particles As Templates



The process involves the infiltration of polyelectrolyte or polymer-drug conjugates into mesoporous shells of SC/MS particles (step 1), followed by cross-linking of the infiltrated polymer chains (step 2) and subsequent removal of the SC/MS silica template (step 3), leading to thick-walled polyelectrolyte or drug-conjugated polymer nanocapsules.

sembled in the capsules can be stabilized via engineered, cleavable covalent linker molecules (e.g., disulfides), which would add tunable stability and degradability characteristics to the capsules, leading to another level of control over the release properties of encapsulated substances.

The monodispersed SC/MS template particles were prepared as reported by Büchel and co-workers.¹⁵ Scanning electron microscopy (SEM) reveals that these particles are homogeneous with a diameter of ca. 420 ± 10 nm (Figure 1a). The particles have a solid core and a mesoporous shell with a shell thickness of ~ 60 nm, as is evident from the transmission electron microscopy (TEM) image (inset, Figure 1a). Nitrogen adsorption data indicated that the SC/MS particles have a surface area of $390 \text{ m}^2 \text{ g}^{-1}$ and an average pore size of 4.5 nm with a pore volume of 0.28 mL g^{-1} .

Poly(allylamine hydrochloride) (PAH) was employed as the first model polyelectrolyte to form polymer nanocapsules. Solutions of PAH with molecular weights of 5000, 15 000, and 70 000 g mol^{-1} (hereafter denoted as PAH-5k, PAH-15k, and PAH-70k, respectively) were infiltrated into the SC/MS particles at pH 8.5. At this pH, PAH adopts a coiled conformation, facilitating its infiltration into the mesoporous shell of the SC/MS particles.¹⁹ The loading of PAH, as estimated by thermogravimetric analysis (TGA), was ca. 110, 65, and 35 mg g^{-1} for the PAH-5k, PAH-15k, and PAH-70k samples, respectively. The higher loading of the lower molecular weight PAH was also observed by a decrease in the surface area from $390 \text{ m}^2 \text{ g}^{-1}$ for pristine SC/MS particles to 160, 230, and $290 \text{ m}^2 \text{ g}^{-1}$ after loading with 5k, 15k, and 70k PAH, respectively. Under the same conditions, a loading of $\sim 7 \text{ mg g}^{-1}$ was obtained for the PAH-5k with nonporous silica spheres of 500 nm diameter, which demonstrates the potential of the SC/MS particles to achieve significantly higher loadings (>1 order of magnitude).

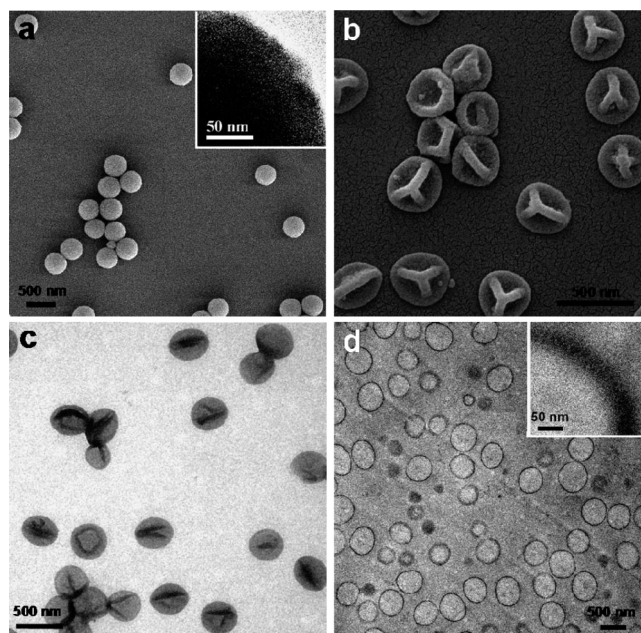


Figure 1. SEM (a) and TEM (inset in a) images of the SC/MS template particles. SEM (b), TEM (c), and ultramicrotomed TEM (d) images of PAH-15k nanocapsules, prepared using the SC/MS template particles and after template removal. The inset in (d) shows a higher magnification image of the capsule shell.

The PAH molecules, assembled in the mesoporous shells of the SC/MS template particles were stabilized using glutaraldehyde (GA) as a cross-linking agent. After cross-linking, the SC/MS template particles were removed via treatment with hydrofluoric acid to obtain PAH nanocapsules with a ζ -potential of +35 mV, compared to -32 mV for the SC/MS template particles. SEM and TEM analysis revealed that the individual nanocapsules formed using PAH-15k are $\sim 370 \pm 10$ nm in diameter (parts b and c of Figure 1), approximately 12% smaller than the template particles used. The capsules preserve their structural integrity and show significantly fewer folds and creases than those typically found in polymer capsules prepared by the LbL procedure.^{6,9} This is likely to be caused by the relatively small size of the capsules and the thick capsule shells. In addition, cross-linking in the shell provides extra mechanical strength and enhances the stability of the capsules formed. The structure of the capsules was further examined by TEM analysis of ultramicrotomed sections (90 nm thin slices) of the capsules (Figure 1d). The apparent heterogeneity in capsule size (100–500 nm) in the ultramicrotomed sample is due to the slicing of the capsules through random sections. In addition, a slight increase in capsule size ($\sim 25\%$) is observed, which is likely to be caused by the swelling of the capsules during sample preparation, which requires setting them in a resin before microtoming (Figure 1d). At higher magnification, a uniform shell is clearly seen (inset, Figure 1d), confirming the structural integrity of the capsule shells. The PAH-15k capsule shell, assembled by a single polymer adsorption step, has a thickness of 27 ± 3 nm, which is more than 10 times thicker than the average increment of one PAH layer (~ 2 nm) deposited on nonporous particles via LbL assembly.^{6,8,9} The thickness of the capsule shells

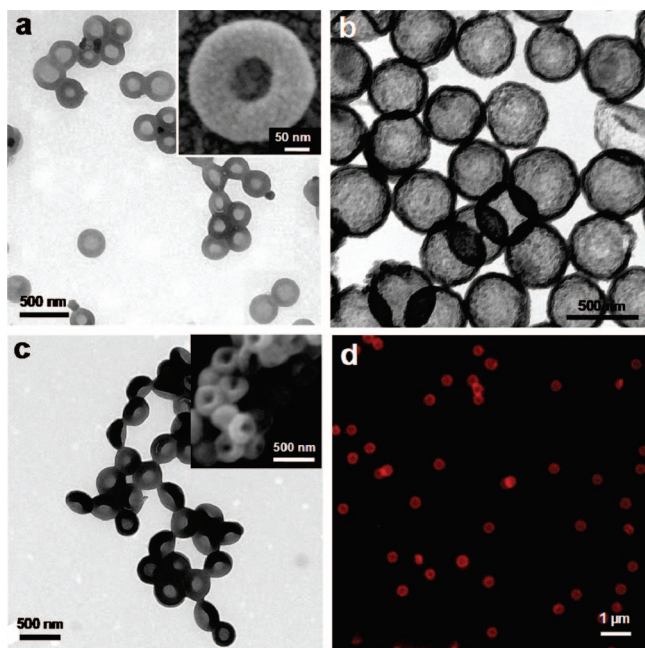


Figure 2. PLL (a, b) and PGA-Dox (c, d) nanocapsules formed using SC/MS template. The cross-linking agents used are GA (a), DMDTPC (b), and cystamine (c, d), respectively. Panels a–c are TEM images, the insets of panels (a and c) are SEM images, and panel (d) is a fluorescence microscopy image of the nanocapsules. The fluorescence signal of capsules in panel d arises from Dox in the capsules.

increases as the molecular weight of the PAH decreases: ~ 45 nm and ~ 16 nm were obtained for PAH of 5 kDa and 70 kDa, respectively (data not shown). This correlates well to the more efficient adsorption of smaller PAH in the mesoporous shells described above.

For drug delivery applications, we explored the preparation of polymer capsules according to the outlined approach using polymers that are structurally related to natural proteins and are generally considered to be biocompatible and biodegradable,²⁰ namely, poly(L-amino acids): cationic poly(L-lysine) and anionic poly(L-glutamic acid). Positively charged poly(L-lysine) (PLL, M_w 1000–4000 g mol⁻¹) capsules, with a homogeneous size distribution, were prepared by a one-step PLL assembly in the SC/MS template, followed by GA cross-linking and removal of the SC/MS template. TEM analysis of the PLL capsules showed a ringlike morphology, with a diameter of 270 ± 10 nm (Figure 2a), representing $\sim 36\%$ shrinkage from the original template particle size. From TEM, the shell thickness was 50 nm. The integrity of the capsules was confirmed by SEM, which showed a donut-like morphology (inset, Figure 2a).

This technique can also be extended to prepare capsules with various cross-linking reagents, which makes the capsule properties tunable for different applications. For instance, dimethyl 3,3'-dithiopropionimidate dihydrochloride (DMDTPC) is a homobifunctional cross-linking agent used to cross-link proteins and peptides through the formation of amidine bonds via the amine groups. The formed amidine bond retains the net charge character of the protein or peptide to be cross-linked, and the DMDTPC can also provide a cleavable disulfide bond in the capsule shell. Figure 2b shows

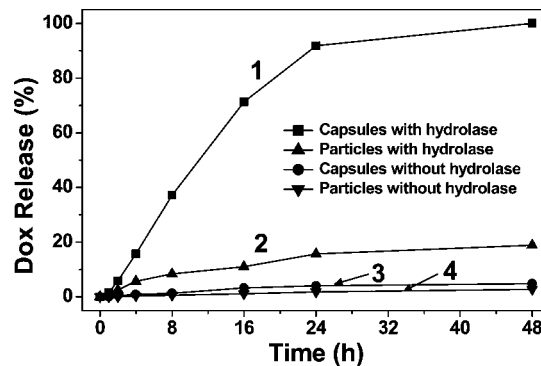


Figure 3. In vitro release studies from PGA-Dox particles and capsules in the presence of 10 mM carboxypeptidase (pH 5.8) (curves 1 and 2) and in the absence of external hydrolase (pH 7.4) (curves 3 and 4).

a TEM image of the PLL (M_w 40–60 kDa) capsules prepared using DMDTPC as a cross-linker. The intact PLL capsules showed a ringlike morphology with a diameter of 400 ± 10 nm and a shell thickness of 40 nm.

Among various poly(L-amino acids), the negatively charged poly(γ -substituted glutamic acid) derivatives have been found to be promising polymer materials for biomedical applications due to their biocompatible, nonimmunogenic, and biodegradable nature.^{20,21} Here, the amine-functionalized positively charged SC/MS particles were used to adsorb poly(L-glutamic acid) (PGA, M_w 1500–3000 g mol⁻¹) conjugated with the model anticancer drug, doxorubicin (Dox). The polymer–drug conjugate, PGA-Dox, was loaded in the mesoporous shells and cross-linked using 2,2'-diaminodiethyl disulfide dihydrochloride (cystamine) in the presence of 1-ethyl-3-(3-dimethylaminopropyl) carbodiimide hydrochloride. After removal of the SC/MS template, PGA-Dox nanocapsules with a homogeneous size distribution were obtained (Figure 2c–d). The capsules are thick-walled (55–60 nm) and have an average diameter of ~ 370 nm. As visualized by fluorescence microscopy, the resulting capsules were well-dispersed in PBS (pH 7.4) and resembled the shape and size of the SC/MS particles (Figure 2d).

As an initial test to verify the utility of the obtained PGA-Dox capsules for drug delivery applications, PGA-Dox SC/MS particles (hereafter referred to as PGA-Dox particles) and PGA-Dox capsules were subjected to in vitro degradation and Dox release at conditions resembling those within living cells. The physiological pH of the blood stream is 7.4, while subcellular lysosomal compartments (endosomes and lysosomes) of tumor cells have reducing environments and possess several hydrolytic enzymes at acidic pH ($\text{pH} \leq 5.8$). For a drug delivery vehicle to be highly effective, it is desirable that it should not degrade in the blood stream; however, it should be easily degraded and release its cargo after reaching the lysosomal compartments of the tumor cells. The PGA-Dox particles and capsules were exposed to 10 mM carboxypeptidase at 37 °C in 100 mM PBS (pH 5.8), which can cleave the amide bonds in PGA-Dox. PGA-Dox capsules were gradually degraded in the presence of a carboxypeptidase with near-linear drug release kinetics over the first 24 h (curve 1, Figure 3). In comparison, significantly

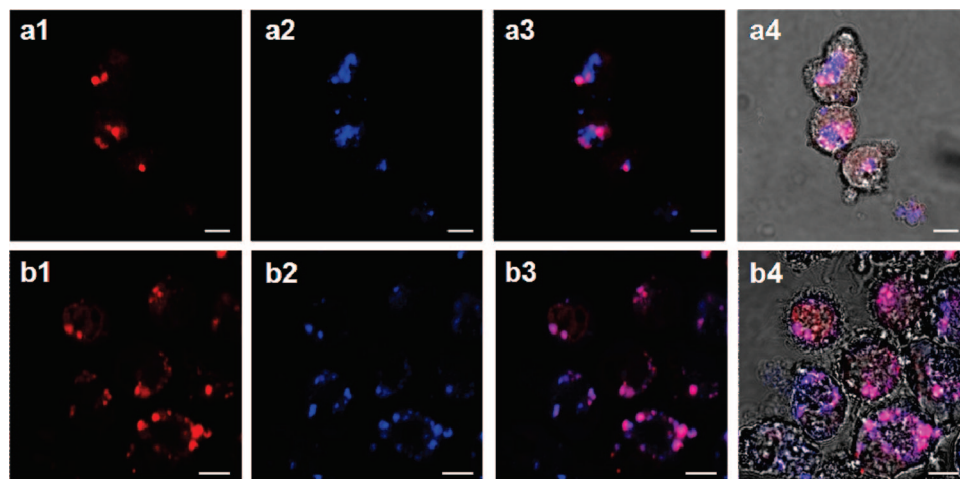


Figure 4. CLSM images showing the uptake of PGA-Dox particles (a1–a4) and PGA-Dox capsules (b1–b4) by LIM1215 colorectal tumor cells. The images show the fluorescent signals arising from doxorubicin (a1, b1), Lysotracker Blue lysosomal dye (a2, b2), merged images of doxorubicin and Lysotracker Blue signals (a3, b3), and merged images of doxorubicin, Lysotracker Blue, and phase contrast signals (a4, b4). The scale bars correspond to 10 μm .

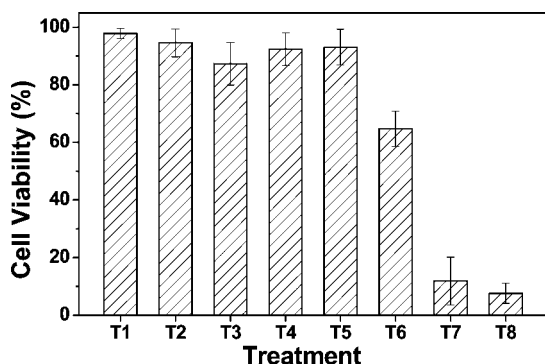


Figure 5. Trypan blue cell viability assay showing the percentage viability of LIM1215 human colorectal tumor cells in the absence of any external agent (T1) and in the presence of PGA polymer (T2), PGA particles (T3), PGA capsules (T4), PGA-Dox polymer conjugates (T5), PGA-Dox particles (T6), PGA-Dox capsules (T7), and free Dox (T8), after 16 h of treatment. The results shown represent the average of three independent experiments.

less Dox was released from PGA-Dox particles in the presence of carboxypeptidase (<20% Dox release in 48 h) (curve 2, Figure 3), probably due to limited access of carboxypeptidase to the polymer. Negligible passive release of Dox was observed when particles/capsules were exposed to 100 mM PBS, in the absence of any external hydrolase at pH 7.4 (curves 3 and 4, Figure 3) and pH 5.8 (data not shown). It is noteworthy that these *in vitro* experiments were performed under nonreducing conditions, however, it is expected that the reducing environments in the lysosomal compartments of the tumors will further facilitate the disassembly (breakdown) of PGA-Dox capsules via cleavage of the disulfide bond in the cystamine linker used in the assembly of PGA-Dox capsules.²²

The results obtained from *in vitro* Dox-release studies motivated us to further investigate the uptake of PGA-Dox particles and capsules by LIM1215 human colorectal tumor cells. The size of the particles/capsules (<500 nm) studied here is within the range capable of exploiting the “leaky” nature of tumor blood vessels, which have pore diameters

of between 400 and 600 nm,²³ allowing accessibility to target tumor cells. Confocal microscopy images of LIM1215 colorectal tumor cells incubated with PGA-Dox particles (Figure 4a) and capsules (Figure 4b) for 16 h show internalization of both particles and capsules, with nearly all the cells containing particles/capsules. Most of the internalized particles/capsules are taken up by the lysosomes, as is evident from the merged confocal images (Figure 4, a3 and b3), showing the colocalization of fluorescence signals arising from Dox (Figure 4, a1 and b1) and Lysotracker Blue, a lysosome staining dye (Figure 4, a2 and b2). The uptake of the PGA-Dox particles and capsules by subcellular lysosomes suggests that once internalized, hydrolytic enzymes present in the reducing environment of the lysosomes would facilitate Dox release, thus causing tumor cell death.

The ability of PGA-Dox particles and capsules to cause death of LIM1215 tumor cells was investigated using a trypan blue cell viability assay (Figure 5). For the cell viability assays, the LIM1215 tumor cells were treated with an equal number of particles/capsules per cell (T3, T4, T6, and T7, Figure 5). The various controls (T2, T5, and T8, Figure 5) contained at least an equivalent amount of PGA and/or Dox present in the particles/capsules (see Supporting Information for details). PGA polymer (T2, Figure 5), PGA particles (T3, Figure 5), and PGA capsules (T4, Figure 5) did not significantly affect the cell viability, suggesting that PGA is biocompatible in free polymer form as well as in the form of particles or capsules.^{20,21} Conversely, treatment of LIM1215 colorectal tumor cells with PGA-Dox particles (T6, Figure 5) and PGA-Dox capsules (T7, Figure 5) resulted in a significant decrease in the number of viable tumor cells. The PGA-Dox capsules were found to be more effective in eradicating the tumor cells (>85% cell death) than PGA-Dox particles (<40% cell death) within 16 h, which corroborates well with the *in vitro* Dox-release studies (Figure 3). Interestingly, when LIM1215 tumor cells were treated with PGA-Dox polymer conjugates, insignificant

tumor cell death was observed (T5, Figure 5). These results are also in agreement with previous reports wherein PGA-Dox polymer conjugates were found to be almost totally devoid of cell growth-inhibiting activities during in vitro studies.²⁴ We speculate that the high negative charge of the small PGA-Dox polymer chains restricts their uptake by the negatively charged cell membranes and hence leads to reduced cell death. However, PGA-Dox particles and capsules can be internalized into the tumor cells via endocytosis due to their larger sizes,²⁵ thus highlighting the important role that polymer capsules might play in drug delivery applications. We note that although free Dox (T8, Figure 5) is as efficient as PGA-Dox capsules (T7, Figure 5) in causing tumor cell death, Dox is known to cause high systemic toxicity when administered into animals in its free form.²⁶ The PGA-Dox capsules, as shown here can provide an added advantage of controlled release, wherein Dox molecules will be released only after capsules reach the target tumor site, minimizing any systemic toxicity. Moreover, significantly higher amounts and more than one type of drug can be principally loaded in PGA capsules in a controlled manner, due to the presence of a large number of free $-\text{COOH}$ groups. In addition, the remaining free $-\text{COOH}$ groups of PGA-Dox capsules can be easily conjugated to targeting moieties to target PGA-Dox capsules to various tumors,²⁷ which is the subject of further investigation.

In summary, we report a novel and general technique for the assembly of macromolecules in SC/MS template particles and the subsequent formation of monodispersed, single-component, polymer capsules after removal of the silica templates. Capsules with diameters ranging from ca. 270 to 400 nm, and with shell thicknesses ranging from ca. 15 to 60 nm have been prepared using SC/MS template particles and polymers with varied functionality and molecular weights, as well as cross-linking reagents. The shell thickness of the capsules is found to be governed by the nature and the molecular weight of the macromolecule. PGA-Dox capsules were prepared and represent a unique drug delivery system: they remain stable at physiological pH and are amenable to deconstruction (by disassembly of PGA-Dox chains due to lysosomal reducing environments) and degradation (by lysosomal hydrolases) in response to chemical stimuli within living cells, thereby delivering Dox to LIM1215 human colorectal tumor cells and causing tumor cell death. The attachment of targeting ligands to the drug-conjugated capsules through established coupling protocols will further provide functional capsules for targeted drug delivery applications. Overall, the simple, efficient, and general nature of the approach, coupled with the capability to synthesize a wide range of materials with tunable properties and the additional ability to postfunctionalize the thick capsule shells, provide exciting new opportunities for

designing advanced capsules for use in a range of therapeutic and diagnostic applications.

Acknowledgment. This work was supported by the Australian Research Council under the Federation Fellowship (FC), Australian Postdoctoral Fellowship (ANZ), and Discovery Project FC and ANZ schemes, and by the National Health and Medical Research Council Project Grant 433613 (FC). The Particulate Fluids Processing Centre is acknowledged for infrastructure support and the Ludwig Institute for Cancer Research, Parkville for access to tissue culture facilities. Dr. Almar Postma is thanked for assistance with the SEM measurements.

Supporting Information Available: Details of the experimental procedures and cellular experiments. This material is available free of charge via the Internet at <http://pubs.acs.org>.

References

- (1) Duncan, R. *Nat. Rev. Drug Discovery* **2003**, *2*, 347.
- (2) Kiick, K. L. *Science* **2007**, *317*, 1182.
- (3) Uhrich, K. E.; Cannizzaro, S. M.; Langer, R. S.; Shakesheff, K. M. *Chem. Rev.* **1999**, *99*, 3181.
- (4) Discher, B. M.; Won, Y.; Ege, D. S.; Lee, J. C.; Bates, F. S.; Discher, D. E.; Hamner, D. A. *Science* **1999**, *284*, 1143.
- (5) Thurmond, K. B.; Kowalewski, T.; Wooley, K. L. *J. Am. Chem. Soc.* **1997**, *119*, 6656.
- (6) Peyratout, C. S.; Dähne, L. *Angew. Chem., Int. Ed.* **2004**, *43*, 3762.
- (7) Wang, Y.; Angelatos, A. S.; Caruso, F. *Chem. Mater.* **2008**, *20*, 848.
- (8) Caruso, F.; Caruso, R. A.; Möhwald, H. *Science* **1998**, *282*, 1111.
- (9) Donath, E.; Sukhorukov, G. B.; Caruso, F.; Davis, S. A.; Möhwald, H. *Angew. Chem., Int. Ed.* **1998**, *37*, 2201.
- (10) Quinn, J. F.; Johnston, A. P. R.; Such, G. K.; Zelikin, A. N.; Caruso, F. *Chem. Soc. Rev.* **2007**, *36*, 707.
- (11) Volodkin, V.; Petrov, A. I.; Prevot, M.; Sukhorukov, G. B. *Langmuir* **2004**, *20*, 3398.
- (12) Wang, Y.; Yu, A.; Caruso, F. *Angew. Chem., Int. Ed.* **2005**, *44*, 2888.
- (13) Wang, Y.; Caruso, F. *Adv. Mater.* **2006**, *18*, 795.
- (14) Wang, Y.; Caruso, F. *Chem. Mater.* **2006**, *18*, 4089.
- (15) Büchel, G.; Unger, K. K.; Matsumoto, A.; Tsutsumi, K. *Adv. Mater.* **1998**, *10*, 1036.
- (16) Kim, M.; Yoon, S. B.; Sohn, K.; Kim, J. Y.; Shin, C. H.; Hyeon, T.; Yu, J. S. *Microporous Mesoporous Mater.* **2003**, *63*, 1.
- (17) Kim, J. Y.; Yoon, S. B.; Yu, J. S. *Chem. Commun.* **2003**, 790.
- (18) Zhao, W. R.; Gu, J. L.; Zhang, L. X.; Chen, H. R.; Shi, J. L. *J. Am. Chem. Soc.* **2005**, *127*, 8917.
- (19) Angelatos, A. S.; Wang, Y.; Caruso, F. *Langmuir* **2008**, *24*, 4224.
- (20) Khandare, J.; Minko, T. *Prog. Polym. Sci.* **2006**, *359*.
- (21) Li, Chun. *Adv. Drug. Delivery Rev.* **2002**, *54*, 695.
- (22) Saito, G.; Swanson, J. A.; Lee, K. *Adv. Drug Delivery Rev.* **2003**, *55*, 199.
- (23) Yuan, F.; Dellian, M.; Fukumura, D.; Leunig, M.; Berk, D. A.; Torchilin, V. P.; Jain, R. K. *Cancer Res.* **1995**, *55*, 3752.
- (24) Hoes, C. J. T.; Potman, W.; van Heeswijk, W. A. R.; Mud, J.; de Grooth, B. G.; Greve, J.; Feijen, J. *J. Controlled Release* **1985**, *2*, 205.
- (25) Kohane, D. S. *Biotechnol. Bioeng.* **2007**, *96*, 203.
- (26) O'Keefe, D. A.; Sisson, D. D.; Gelberg, H. B.; Schaeffer, D. J.; Krawiec, D. R. *J. Vet. Intern. Med.* **1993**, *7*, 309.
- (27) Cortez, C.; Tomaskovic-Crook, E.; Johnston, A. P. R.; Radt, B.; Cody, S. H.; Scott, A. M.; Nice, E. C.; Heath, J. K.; Caruso, F. *Adv. Mater.* **2006**, *18*, 1998.

NL080877C